INVESTIGATION ON THE IMPACT OF CARBON NANOPLATELETS ON THE THERMAL BEHAVIOR OF MAGNESIUM COMPOSITES

by

Mohammed A. ALMESHAAL[a], Govindasamy MAHENDRAN[b*], A. CHANDRASHEKHAR[c], Sumanth Ratna KANDAVALLI[d], Ravishankar SATHYAMURTHY[e], Ramasamy BALAMURUGAN[f], Gurusamy PUTHILIBAI[g], Vijayan VENKATRAMAN[h*], and Ramkumar KATHALINGAM[i]

[a] Department of Mechanical Engineering,
College of Engineering Imam Mohammad Ibn Saud,
Islamic University, Riyadh, Saudi Arabia
[b] Department of Mechanical Engineering, R.M.K Engineering College,
Kavaraipettai, Tamil Nadu, India
[c] Department of Mechanical Engineering, Faculty of Science and Technology,
ICFAI Foundation for Higher Education, Hyderabad, Telangana, India
[d] Department of Mechanical Engineering, Tandon School of Engineering,
New York University, Brooklyn, New York, USA
[e] Department of Mechanical Engineering,
Interdisciplinary Research Center for Renewable Energy and Power Systems (IRC-REPS),
King Fahd University of Petroleum and Minerals,
Dhahran, Saudi Arabia
[f] Department of Mechanical Engineering,
M. Kumarasamy College of Engineering, Karur, Tamil Nadu, India
[g] Department of Chemistry, Sri Sairam Engineering College,
Chennai, Tamil Nadu, India
[h] Department of Mechanical Engineering, K. Ramakrishnan College of Technology,
Tiruchirappalli, India
[i] Department of Mechanical Engineering, School of Engineering and Technology,
Dhanalakshmi Srinivasan University, Tiruchirappalli, Tamil Nadu, India

Original scientific paper
https://doi.org/10.2298/TSCI230322004A

The Mg/2.4 wt.% CNP composite has a specific heat capacity improvement of 174%, according to DSC testing results. The TGA data reveals a 2.4% decrease in mass when comparing the Mg/2.4 wt.% CNP composite to pure Mg. The coefficient of heat transfer, the effectiveness of the fin, and the heat conduction via fin were all evaluated with a pin-fin transferring of heat under conditions of both free and forced convection. When carbon nanoplatelets are added to a Mg matrix, the resulting composites have better heat transfer characteristics when subjected to both natural and artificial convection.

Key words: *carbon nanoplatelets, fin efficiency, magnesium composites, heat transfer rate, heat transfer characteristics*

* Corresponding author, e-mail: vijayan.me@gmail.com

Introduction

The increasing use of traditional fossil fuels to supply industrial energy needs has resulted in significant environmental contamination, but energy is essential for global economic advancement and industrialization [1]. Reducing thermal energy losses in energy-consuming equipment is essential to finding solutions to these energy issues. The Cu, Ag, and Mg are just a few examples of the many technical uses for materials with high thermal conductivity, which allow for the efficient transfer of heat. Producing electricity, heating and cooling systems, transportation, aviation, electronics, and more are all examples. The Mg, in particular, is a favourite due to its versatility and low price [2, 3].

Composites, which are made by combining several materials with a matrix material, are typically employed in specialised contexts. Metal matrix composites (MMC) exhibit exceptional characteristics that make them highly suitable for applications across structural, mechanical, and thermal sectors [4]. The MMC are reinforced with materials including ZrO_2, B_4C, Al_2O_3, SiC, BN, TiB_2, TiC, carbon nanotubes (CNT), and graphene to improve their stability, advantageous strength-to-weight ratio, efficient thermal conduction, and corrosive resistance under elevated temperatures. In particular, aluminum matrix composites incorporating CNT and graphene have garnered significant interest due to their superior mechanical and thermal properties [5].

The production of Mg composites reinforced with CNT and graphene presents particular challenges for heat transfer applications, primarily because of the reactive nature of these materials at the temperatures required for processing [6]. To address these issues, manufacturing methods such as powder metallurgy followed by hot extrusion are preferred, as they help circumvent the reactivity problems. In the context of powder metallurgy, the formability of the material is critical, especially when crafting heat transfer fins from CNT and graphene-reinforced Mg composites [7]. Graphene nanoplatelets, in particular, have shown to have an edge over CNT regarding their mechanical and thermal conductivity.

The focus of the present research is to delve into the thermal conductivity attributes of graphene nanoplatelet-reinforced Mg composites. Prior studies [8] have assessed the mechanical properties of both pure Mg and Mg composites fortified with graphene oxide, revealing a substantial 28.64% enhancement in microhardness for Mg composites with a 0.2 wt.% of graphene oxide compared to the pure metal.

Furthermore, investigations [9] into thermal management within electronic systems using graphene nanoplatelets have demonstrated promising results. The incorporation of graphene nanoplatelets into the Mg matrix has been found to enhance thermal properties, showcasing their potential as efficient thermal interface materials.

Researchers [10] used deformation-driven metallurgy to find the optimal blend of strength and ductility in graphene nanoplatelets-dispersed Mg composites. These composites were found to have a tensile strength 317% higher than pure Mg, but a ductility 27% lower. Using the accumulating roll bonding technique, researchers [11] created graphene oxide-dispersed Mg composites, which enhanced microhardness by up to 14% relative to the base material. Increasing the number of rolls has an effect on the difficulty, they found.

Using chemical vapour deposition and hot pressing, Thiangviriya *et al*. [12] investigated composites with scattered graphene nanoplatelets. Based on their findings, a composite containing 3.3% vol.% graphene nanoplatelets significantly improved in both heat conductivity (by 96.8%) and flexural strength (by 122%). Deformation and fracture in graphene-reinforced magnesium composites were studied in a simulation research [13] using finite element analysis. The results of the finite element analysis were found to be in agreement with the experimental and theoretical findings. The thermal behaviour of graphene-reinforced magnesium composites

was studied by the authors [14] in both static and dynamic conditions. They found that the performance of the composite improved up to a graphene level of 2% by volume, but dropped off significantly above this threshold.

The effects of variations in critical temperature were modelled, along with those of changes in geometry and mechanical and physical properties of the material. The authors [15] looked at the high temperature stabilization of a CNT-dispersed Mg composite. Their outcome showed that after annealing at 500 °C, the composite retained around 94% of its initial hardness. The composites' tensile strength even surpassed that of pure Mg at higher temperatures. Because of the interfacial interaction between the graphene and the Mg matrix, they found that the material was thermally stable.

Graphene nanoplatelets dispersed in Mg composites have been studied for their micro-structure and mechanical properties using powder metallurgy, but hot rolling and extrusion have been given far less attention. The objective of this research is to measure the coefficient of heat transfer, the rate of heat transfer, and the efficiency of fins composed of hot-extruded Mg composites that have been enhanced with graphene nanoplatelets, within thermal management systems. These parameters will be quantified to evaluate the effectiveness of the graphene-reinforced Mg material in dissipating heat.

Methodology

Preparation of composites

Powder metallurgy followed by hot extrusion is used to make carbon nanoplatelet (CNP) scattered Mg composites with uniform reinforcement throughout the matrix. The Mg and CNP are the fundamental elements of the unadulterated raw materials used to make these composites. Detailed instructions for making composites from scattered CNP and MgO are provided.

Evaluation of properties for carbon-dispersed magnesium composites

Figure 1 is a diagram of a pin-fin heat exchanger, which is used to determine the fin efficiency (FE), heat transfer rate (HTR), and heat transfer coefficient (HTC). Hot extruded magnesium composites are machined into 13 mm diameter and 160 mm span pins for use in the device. An electric heater is integrated into the pin-fin configuration via a pin that facilitates heat dissipation into the surrounding air. Voltmeters and ammeters are used to measure voltage and current, respectively, to track the amount of heat being generated throughout experiments. The duct of the instrument is connected to a *U*-tube manometer for objective measurement. The

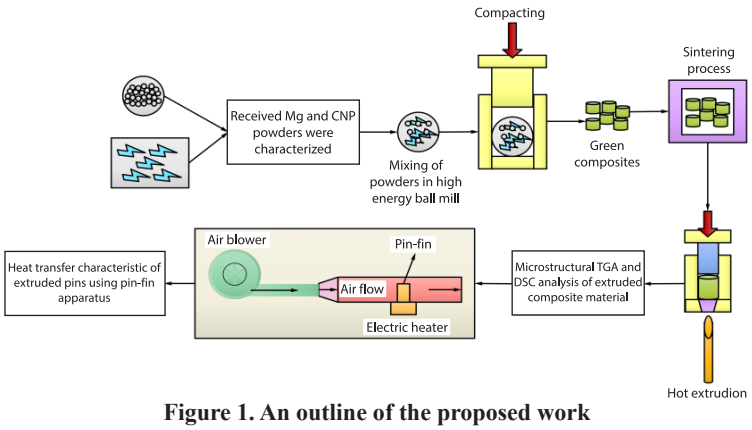

Figure 1. An outline of the proposed work

pin's surface temperatures are measured at many locations by the utilization of *K*-type thermocouples, accompanied by a digital display device that aids in temperature observation. The HTC of the manufactured composites material can be analyzed in both forced and free convection modes thanks to the use of an air blower to manage the environment. The temperature of the pin's surface is measured digitally at five evenly spaced locations under a given voltage and current load. By employing existing empirical formulas and the collected temperature data and thermal conductivity of the composites, the heat transfer parameters are examined.

Components of dispersed Al composites with respect to theoretical heat transfer

Heat transferring factors of carbon-detached Mg composites, like the HTC, the FE, and the HTR, are the primary emphasis of this work, which is based on empirical equations. Another major consideration is the produced composites' thermal conductivity, k [16]:

$$k = \frac{Qt}{A\Delta T} \tag{1}$$

The HTR is determined by:

$$Q = VI \tag{2}$$

From, T_b and T_o we can calculate the temperature difference:

$$\Delta T = T_b - T_o \tag{3}$$

When investigating free convection, turn off the air blower. Hot and cold air have different densities and temperatures, thus they push and pull against one another within the duct. The eqs. (4) and (5) are used to calculate the wall and film temperatures eq. (5) [17]:

$$T_w = \frac{T_1 + T_2 + T_3 + T_4 + T_5}{5} \tag{4}$$

$$T_f = \frac{T_b + T_w}{2} \tag{5}$$

The selection of fluid properties such as Prandtl number, density, viscosity, *etc.*, is based on the film temperature. Flow properties are calculated using the Grashof number:

$$\mathrm{Gr} = \frac{\mathrm{g}\beta\Delta TL^3}{\vartheta^2} \tag{6}$$

The Nusselt number is a dimensional factor defined, and it is used to identify the major method of heat transport by convection [18]:

$$\mathrm{Nu} = 0.63(\mathrm{GrPr})^{0.25} \tag{7}$$

Forced convection heating is achieved by circulating air around the duct. Temperature measurements taken at different pins are used, just as they are in free convection, to determine the HTC. Fluid properties such as viscosity, density, and Prandtl number, among others, are determined based on the film temperature. In forced convection, the Reynolds number, describes the fluid movement:

$$\mathrm{Re} = \frac{Vd}{\vartheta} \tag{8}$$

From the preceding eq. (7), the convective HTC, h, may be determined [19]:

$$h = \frac{\mathrm{Nu}k}{d} \tag{9}$$

Equation can be used to calculate the fluid's velocity (10):

$$V = \frac{v}{A} \tag{10}$$

The flow rate of fluid volume, v, needed to get the velocity:

$$v = \left\{ 0.64 \frac{\pi}{4} d^2 \sqrt{\left(2gH_a\right)} \right\} \tag{11}$$

The air pressure head can be determined using the U-tube manometer:

$$H_a = H_w \frac{\rho_w}{\rho_a} \tag{12}$$

The eq. (13) can be used to determine the water pressure head in the U-tube manometer:

$$H_w = \frac{\frac{h_2}{2} + h_1}{\rho_w} \tag{13}$$

For forced convection, the Nusselt number is defined:

$$\mathrm{Nu} = 0.93\mathrm{Re}^{0.618}\mathrm{Pr}^{0.333} \tag{14}$$

As with free convection, eq. (15) can be used to determine the convective HTC:

$$h = \frac{\mathrm{Nu}k}{d} \tag{15}$$

The FE, η_{fin}, is just as crucial as the convective HTC. The FE is measured by how much heat it can actually transport compared to how much heat it can transfer while still keeping the ambient temperature constant:

$$\eta_{\mathrm{fin}} = \frac{\tanh\left(mL\right)}{mL} \tag{16}$$

$$m = \sqrt{\frac{hP}{kA}} \tag{17}$$

Compared to a flat surface, the increased HTR attained by a fin is represented by its rate of heat transfer, Q_{fin} [20]:

$$Q_{\mathrm{fin}} = \sqrt{hPkA}\left(T_w - T_b\right)\tanh\left(mL\right) \tag{18}$$

Results and discussion

The Mg and carbon content were both detected in the samples analysed using the energy dispersive X-ray (EDX). The majority of the particles in the samples were either Mg nanoplatelets (71.2%) or CNP (88.8%), as seen by the peaks at these percentages in the corresponding EDX images. There is no evidence of impurities in the Mg and CNP powders. The distribution of CNP within the Mg matrix is consistent and exhibits isotropic properties. The use of hot extrusion disperse CNP is an effective method that enhances secondary particle distribution within the matrix.

The results of the DSC predictions for the prepared samples are shown in fig. 3. Specific heat capacities range from 1.990 J/kgK for pure magnesium to 2.430 J/kgK for Mg/0.6 wt.% CNP to 3.158 J/kgK for Mg/1.2 wt.% CNP to 4.208 J/kgK for Mg/2.4 wt.% CNP. The capability to store energy is greatly affected by the specific heat capacity. Therefore, Mg compos-

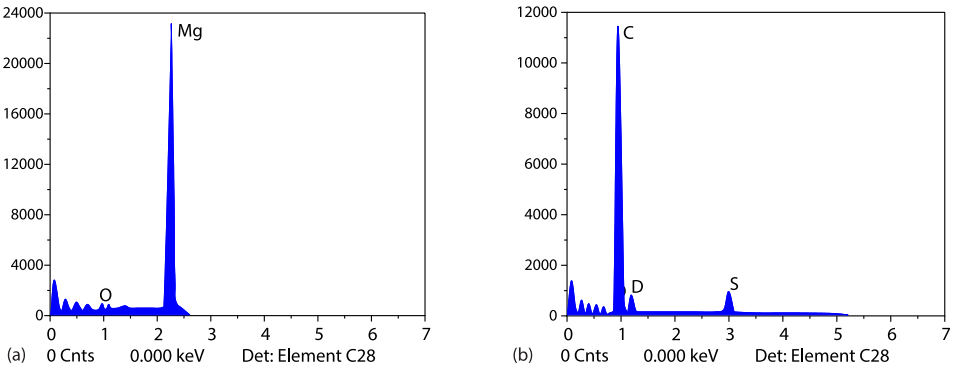

Figure 2. The EDX scans of (a) the pure Mg powder and (b) the CNP

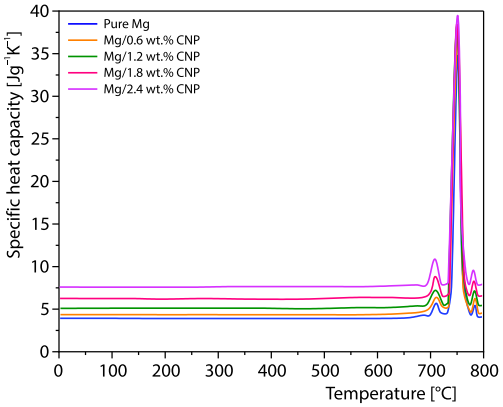

Figure 3. The effect of carbon dispersion on the specific heat capacity of Mg composites

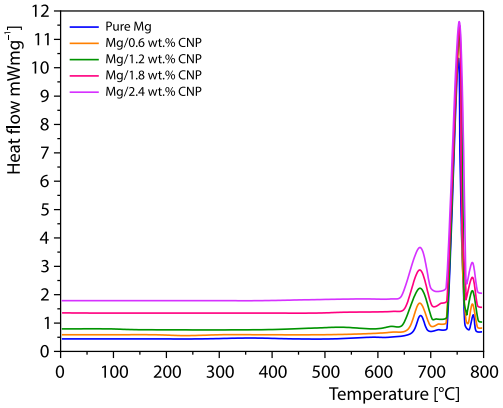

Figure 4. The DSC plot of the carbon-dispersed Mg composites after preparation

ites with added CNP are more suited for heat dissipation applications due to their increased specific heat capacity. The Mg/2.4 wt.% CNP composite has a specific heat capacity that is 174% higher than that of pure Mg.

Differential scanning calorimetry readings were taken in a nitrogen atmosphere using a NETZSCH STA 449F3 instrument. Each sample, weighing about 3 g, was heated from 30 °C to 750 °C in an alumina pan at a rate of 25 °C per minute. The DSC thermographs for all of the specimen are shown in fig. 4. Temperature *vs*. heat flow charts for various CNP wt.% dispersed in a Mg matrix are shown in fig. 4. The results show that heat conduction is improved by including CNP into the Mg matrix. The effective heat transmission is mostly due to the phonon-interaction between the CNP and the Mg matrix, which is made possible by the strong contact between the two. In particular, the Mg/2.4 wt.% CNP sample has a heat flow value that is 210% higher than the pure Mg sample.

Mass loss during heating in a nitrogen atmosphere was measured using a TGA to evaluate thermal stability. The samples, each weighing around 5 g, were heated to 700 °C from room temperature. The results indicate that pure Mg exhibits greater thermal stability compared to the composites. As reinforcement is added, the mass reduction during heating increases. At 500 °C, composites made with Mg and 0.6%, 1.2%, and 1.8% CNP all lose less than 2% of their mass, but the Mg/2.4% CNP composite loses a maximum of 2.67% of its mass, fig.

5. Above the average operating temperature for heat exchangers, when mass loss is typically measured, the effect of composition becomes negligible, at around 350 °C. Therefore, CNP as reinforcement in a Mg matrix can be very useful in heat exchangers and other thermal applications.

The Nusselt number, defines the most common types of heat transport, which are conduction and convection. A higher Nusselt number signifies that convection plays a more significant role in heat transfer than conduction. Nusselt number shifts for various loads in forced convection mode are shown in fig. 6. The relative importance of conduction over convection changes as the concentration of reinforcing material in the matrix rises.

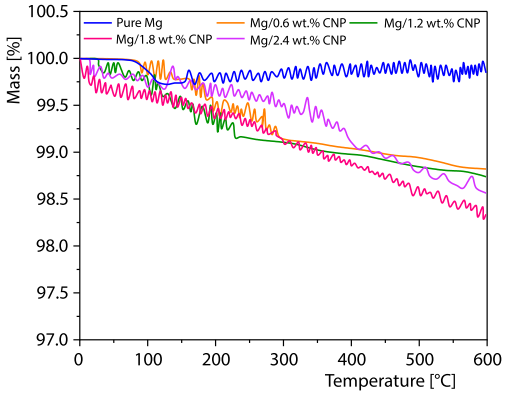

Figure 5. Carbon-dispersed Mg composites using a TGA curve

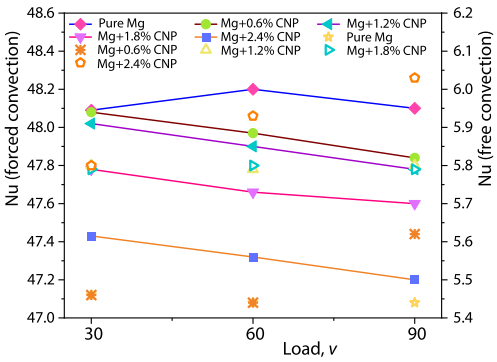

Figure 6. Nusselt number *vs.* load for forced convection and free convection

Pure Mg exhibits a higher Nusselt number compared to all other Mg-CNP composites. When free convection is used as the heat transmission mode, the Nusselt number varies with load as shown in fig. 6. Since there is less fluid contact with the heat source in free convection, the Nusselt number is lower than it is in forced convection. The HTC is a quantity that determines how efficiently energy can be moved from one medium to another, and it is influenced by both the material and fluid properties involved. Figure 9 depicts free convection as well as the range of values for the load-dependent HTC for all materials. The HTC is a proportionality constant affected by the mathematically specified Nusselt number, rendering to Newton's cooling law.

The heat transmission coefficient improves as the Nusselt number rises. As can be seen in fig. 7, the HTC improves when highly conductive reinforcing material is added to the matrix. When comparing a pure Mg sample to a Mg/2.4 wt.% CNP composite, the latter shows a higher HTC. The Mg by itself, with 0.6 wt.% CNP, with 1.2 wt.% CNP, with 1.8 wt.% CNP, and with 2.4 wt.% CNP has an average HTC of 8.353 W/m^{2}K, followed by 8.483 W/m^{2}K, 9.100 W/m^{2}K, 9.903 W/m^{2}K, and 9.373 W/m^{2}K when operating in free convection mode. The HTC is improved by about 19.3% when CNP

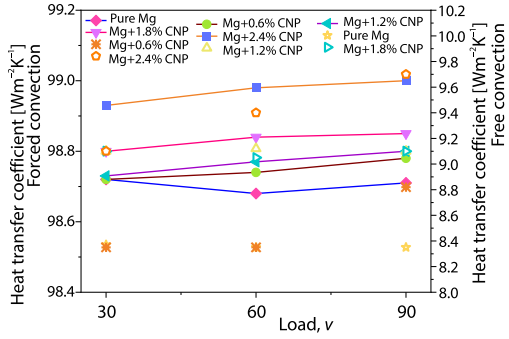

Figure 7. The relationship between load and HTC for forced and free convection

(at a weight percentage of 2.4 wt.%) are incorporated into a Mg matrix. Figure 7 depicts, as a function of heat load, the varying HTC for all compositions susceptible to forced convection. Based on the results of this research, forced convection has a HTC that is around 16 times over than free convection.

The CNP enhance the thermal characteristics of Mg. The Mg, CNP (Mg/0.6 wt.%), Mg (Mg/1.2 wt.%), Mg (Mg/1.8 wt.%), and Mg (Mg/2.4 wt.%) all have different average HTC values when operating in forced convection mode. In order from lowest to highest, the corresponding CNP are 98.703 W/m^{2}K, 98.747 W/m^{2}K, 98.767 W/m^{2}K, 98.830 W/m^{2}K, and 98.970 W/m^{2}K. The value of the HTC in forced convection will increase by about 1% with the addition of CNP.

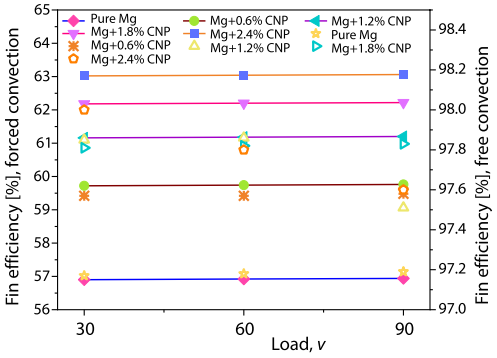

Figure 8. Forced convection and natural-convection FE *vs.* load

Figure 8 depicts the effectiveness of fins under forced conditions for all materials. This efficiency is determined by dividing the actual heat transfer down the length of the fin by the maximum heat transfer that could be achieved while keeping the base temperature constant. A fin's efficiency is proportional to its thermal conductivity. The higher the HTC, the more effective the fins. Under forced convection, the average FE values for pure Mg, Mg/0.6 wt.% CNP, Mg/1.2 wt.% CNP, Mg/1.8 wt.% CNP, and Mg/2.4 wt.% CNP are 59.62%, 59.74%, 61.18%, 62.20%, and 63.04%, respectively. When compared to pure Mg, the effectiveness of fins is improved by about 12% when CNP make up 2.4% of the matrix. Figure 8 displays the relationship between heat load and FE in free convection for all examined compositions. For pure Mg and Mg/0.6 wt.% CNP, Mg/1.2 wt.% CNP, Mg/1.8 wt.% CNP, and Mg/2.4 wt.% CNP, the average FE under free convection is 97.18%, 97.57%, 97.74%, 97.82%, and 97.80%, respectively. When added to a Mg matrix at a concentration of 2.4 wt.%, CNP improve FE by about 1% compared to that of pure Mg.

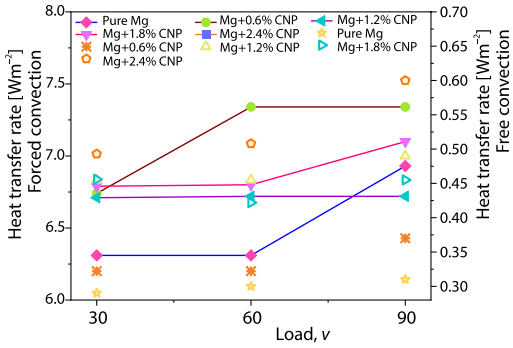

Figure 9. Forced convection heat transfer *vs.* free convection heat transfer under constant load

Figure 9 illustrates the changes in the HTR through the fin as a response to varying heat loads for all the compositions studied. It demonstrates that the heat transfer efficiency in natural or free convection is significantly less effective compared to that in forced convection. The convection HTR is primarily influenced by the HTC. The average HTR recorded by the fin in a free convection scenario are 0.300 W/m^2, 0.338 W/m^2, 0.467 W/m^2, 0.444 W/m^2, and 0.534 W/m^2 for pure Mg, Mg with 0.6 wt.% CNP, Mg with 1.2 wt.% CNP, and Mg with 2.4 wt.% CNP, in ascending order of reinforcement concentration. The HTR was boosted by about 142% when CNP were introduced to Mg at a concentration of 2.4 wt.%.

Figure 9 presents how the HTR through the fin varies with the applied heat load for each composite composition under forced convection conditions. The average HTR by the fin

for pure Mg, Mg with 0.6 wt.% CNP, Mg with 1.2 wt.% CNP, and Mg with 2.4 wt.% CNP under forced convection are recorded at 6.517 W/m^2, 7.14 W/m^2, 6.717 W/m^2, 6.897 W/m^2, and 8.180 W/m^2, respectively. The CNP added to a Mg matrix uniformly and reliably improve thermal conductivity. By incorporating 2.4% by weight of CNP into a Mg matrix, this research demonstrated a 26% increase in heat transmission efficiency.

Conclusion

Powder metallurgy and hot extrusion are used to create CNP-dispersed magnesium composites with improved thermal characteristics and heat transmission. The CNP are dispersed evenly throughout the Mg matrix thanks to the hot extrusion process. The HTC, FE, and HTR were used to assess the heat transfer qualities in both forced and natural-convection conditions. Some of the most noteworthy findings from this experimental research are composites using CNP have been shown to retain their thermal stability when subjected to thermogravimetric testing. The DSC readings demonstrate that the Mg/2.4 wt.% CNP composite has a specific heat capacity that is 174% higher than that of pure Mg. The HTC for Mg/2.4 wt.% CNP indicates improvement of around 1% compared to pure Mg in forced convection and around 18.5% compared to free convection. The FE is increased by 1% in composites containing 2 wt.% CNP distributed in Mg compared to pure Mg, and by 12% in forced convection. When comparing pure Mg to Mg/2.4 wt.% CNP, the difference in HTR is almost 142% in forced convection and 26% in free convection.

References

[1] Plerdsranoy, P., *et a*l., Compaction of $LiBH_4$-MgH_2 doped with MWCNT-TiO_2 for Reversible Hydrogen Storage, *Int. J. Hydrogen Energy*, *42* (2017), 2, pp. 978-986
[2] Sandeep, K. S., *et al*., Operational Control Decisions through Random Rule in Flexible Manufacturing System, in: *Technology Innovation in Mechanical Engineering*: Select Proceedings of TIME 2021, Springer, New York, USA, 2022, pp. 941-950
[3] Kumari, D., *et al*., Numerical Solution of the Effects of Heat and Mass Transfer on Unsteady MHD Free Convection Flow Past an Infinite Vertical Plate, *Frontiers in Heat and Mass Transfer (FHMT)*, *16* (2021), 1, pp. 1-10
[4] Ramya, SD., *et al.*, Performance Study on a Mono-Pass Solar Air Heating System (MPSAH) under the Influence of a PCM, *Mater. Today Proc*., *69* (2022), Part 3, pp. 934-938
[5] Munyalo, J. M., *et al*., Experimental Investigation on Supercooling, Thermal Conductivity and Stability of Nanofluid Based Composite Phase Change Material, *Journal Energy Storage*, *17* (2018), June, pp. 47-55
[6] Ramesh, B., *et al.*, Optimization and Experimental Analysis of Drilling Process Parameters in Radial Drilling Machine for Glass Fiber/Nanogranite Particle Reinforced Epoxy Composites, *Mater. Today Proc.*, *62* (2022), Part 2, pp. 835-840
[7] Pavithra, K. M., *et al*., A Free Convective Two-Phase Flow of Optically Thick Radiative Ternary Hybrid Nanofluid in an Inclined Symmetrical Channel through a Porous Medium, *Symmetry (Basel)*, *15* (2023), 8
[8] Kumar, D. D., *et a*l., Study of Microstructure and Wear Resistance of AA5052/B4C Nanocomposites as a Function of Volume Fraction Reinforcement to Particle Size Ratio by ANN, *Journal Chem.*, *2023* (2023), ID2554098
[9] Rao, M. N., *et al*., Flexible manufacturing System Scheduling through Branch and Bound Algorithm, in: T*echnology Innovation in Mechanical Engineering*: Select Proceedings of TIME 2021, Springer, New York, USA, 2022, pp. 825-836
[10] Munjam, S. R. K., *et a*l., Novel Technique MDDIM Solutions of MHD Flow and Radiative Prandtl-Eyring Fluid over a Stretching Sheet with Convective Heating, *International Journal of Ambient Energy*, *43* (2022), 1, pp. 4850-4859
[11] Sathiaraj, G., *et al*., The Mechanical Behavior of Nanosized Al_2O_3-Reinforced Al-Si7-Mg Alloy Fabricated by Powder Metallurgy and Forging, *ARPN Journal of Engineering and Applied Sciences*, *11* (2016), 9, pp. 6056-6061

[12] Thiangviriya, S., *et al*., The MgH_2-TiF4-MWCNT Based Hydrogen Storage Tank with Central Tube Heat Exchanger, *Int. J. Hydrogen Energy*, *44* (2019), 36, pp. 20173-20182
[13] Girimurugan, R., *et al*., Static and Total Pressure Analysis of Three Way Catalytic Convertor Using CFD, *107* (2022), 1, pp. 7381-7387
[14] Girimurugan, R., *et al.*, Application of Deep Learning to the Prediction of Solar Irradiance through Missing Data, *International Journal of Photoenergy*, *2023* (2023), ID4717110
[15] Kasaeipoor, A., *et al*., Free Convection Heat Transfer and Entropy Generation Analysis of MWCNT-MgO (15% to 85%)/Water nanofluid Using Lattice Boltzmann Method in Cavity with Refrigerant Solid Body-Experimental Thermo-Physical Properties, *Powder Technol*., *322* (2017), Dec., pp. 9-23
[16] Mithran, R., Sadhasivam, C., Experimental studies of pressure drop in compact heat exchanger with aluminum Oxide and Magnesium Oxide, *International Journal of Mechanical and Production Engineering Research and Development*, *9* (2019), 6, pp. 525-534
[17] Amburi, P. K., *et al.*, Novel Use of CuO Nanoparticles Additive for Improving Thermal Conductivity of MgO/Water and MWCNT/Water Nanofluids, *Journal Therm. Anal. Calorim*., *148* (2023), 19, pp. 10389-10398
[18] Khetib, Y., *et al*., The Influence of Forced Convective Heat Transfer on Hybrid Nanofluid-flow in a Heat Exchanger with Elliptical Corrugated Tubes: Numerical Analyses and Optimization, *Applied Sciences (Switzerland)*, *12* (2022), 6
[19] Toudja, N., *et al.*, Thermosolutal Mixed Convection in a Lid-Driven Irregular Hexagon Cavity Filled with MWCNT-MgO (15-85%)/CMC Non-Newtonian Hybrid Nanofluid, *Journal Therm. Anal. Calorim*., 147 (2022), 1, pp. 855-878
[20] Kardam, A., *et al*., Ultrafast Thermal Charging of Inorganic Nanophase Change Material Composites for Solar Thermal Energy Storage, *RSC Adv*., *5* (2015), 70, pp. 56541-56548

Paper submitted: March 22, 2023
Paper revised: September 15, 2023
Paper accepted: October 31, 2023

© 2024 Society of Thermal Engineers of Serbia
Published by the Vinča Institute of Nuclear Sciences, Belgrade, Serbia.
This is an open access article distributed under the CC BY-NC-ND 4.0 terms and conditions